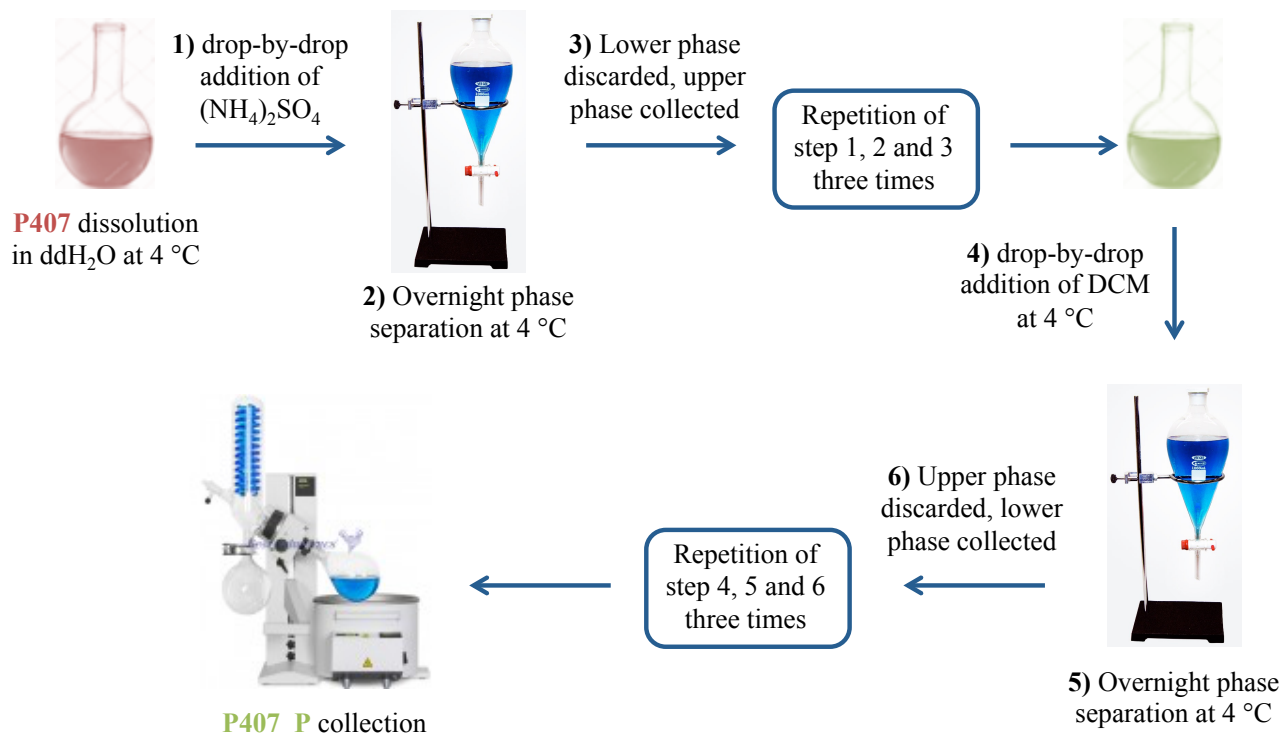


## *Supplementary Material*

### **1 Macrodial purification**

Poloxamer® 407 (P407) purification was carried out according to the method reported by Fakhari et al. with slight modifications [Fakhari et al. 2017]. Briefly, 100 g of P407 were first dissolved in 900 mL of double distilled water (ddH<sub>2</sub>O) under magnetic stirring at 4 °C to avoid micellization phenomena. Then, 1,000 mL of ammonium sulphate ((NH<sub>4</sub>)<sub>2</sub>SO<sub>4</sub>, Carlo Erba Reagents, Italy) solution (25% w/V concentration in ddH<sub>2</sub>O), previously equilibrated at 4 °C and filtered through a 0.22 µm syringe filter (poly(tetrafluoroethylene) membrane, Whatman) were added drop-by-drop to P407 solution under vigorous stirring (figure S1). Subsequently, the turbid solution was transferred to a separation funnel and maintained at 4 °C for 7 h until a complete phase separation was achieved. Then, the lower phase was discarded, while the upper phase was poured into a glass flask and ddH<sub>2</sub>O was added under continuous stirring to reach a final volume of 1 L. 800 mL of cold ammonium sulphate solution, prepared as previously described, were added drop-by-drop to the mixture under vigorous stirring until a turbid solution was observed. This solution was then poured into a separation funnel and kept at 4 °C for 7 h to allow a complete phase separation. The lower phase was discarded, while the upper phase was transferred to a glass flask and cold ddH<sub>2</sub>O was added to reach a final 1 L volume. Then, 800 mL of ammonium sulphate solution were slowly added again to the mixture under vigorous stirring and the turbid solution poured into a separation funnel. After a complete phase separation (7 h at 4 °C), the lower phase was discarded, while the upper phase was transferred to a glass flask and 500 mL of dichloromethane (DCM, Carlo Erba Reagents, Italy) were added drop-by-drop. The mixture was then poured into a separation funnel and kept overnight at 4 °C to allow a complete phase separation. The lower phase was collected, added with 500 mL of DCM, mixed and transferred to a separation funnel. After a complete phase separation, the lower phase was collected into a glass flask and 500 mL of DCM were added again. The solution was then mixed and transferred to a separation funnel to allow phase separation at 4 °C. Finally, the collected lower phase (i.e., the purified Poloxamer® 407, P407\_P) was concentrated under vacuum using a rotary evaporator system (Buchi Rotavapor Labortechnik AG) and dried overnight under the fume hood.



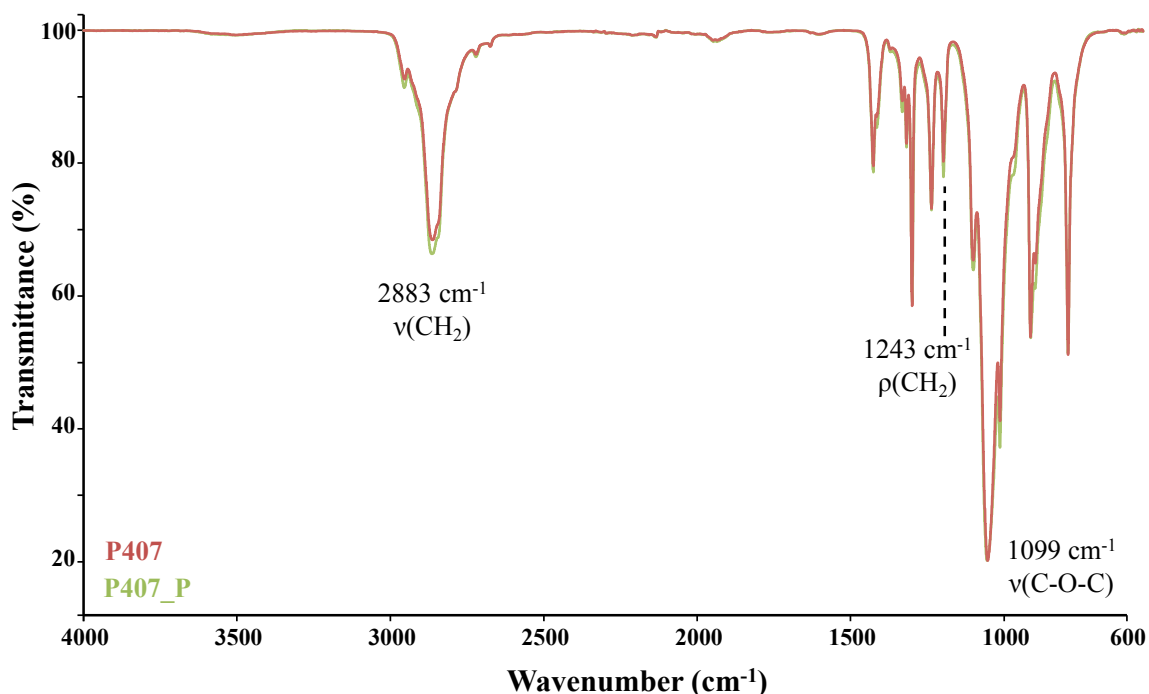
**Supplementary Figure 1.** Schematic representation of the purification procedure performed on Poloxamer® 407 to remove impurities and low molecular weight polymeric chains (i.e., PEO-PPO diblock copolymers).

## 2 Macrodial characterization

The success of the purification procedure performed on the macrodiol was first assessed through Attenuated Total Reflectance Fourier Transform Infrared (ATR-FTIR) spectroscopy and Size Exclusion Chromatography (SEC). Then, the effects resulting from this procedure on hydrogel mechanical properties were investigated through rheological characterization.

### 2.1.1 Chemical characterization

ATR-FTIR spectroscopy was first performed on purified macrodiol (P407\_P) samples to assess the presence of Poloxamer® characteristic vibrational bands after the purification procedure. P407 was also analyzed as control condition and the resulting average spectra are reported in figure S2.



**Supplementary Figure 2.** Average ATR-FTIR spectra of P407 as such (red) and purified P407 (P407\_P) (green).

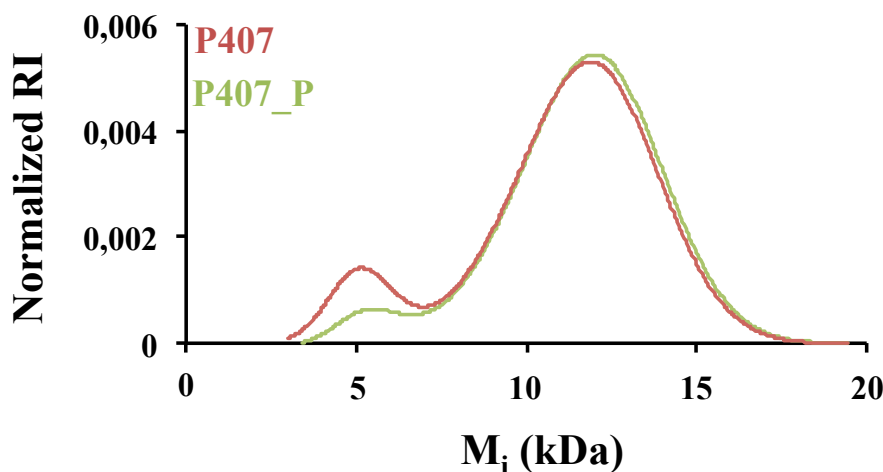
Both spectra showed the characteristic vibrational bands at  $2,883\text{ cm}^{-1}$  and  $1,243\text{ cm}^{-1}$  ascribed to the  $\text{CH}_2$  stretching and rocking vibrations, respectively. Moreover, the band at  $1,099\text{ cm}^{-1}$  was attributed to the stretching vibration of the C-O-C repeating units, according to the work published by Boffito et al. [Boffito et al. 2016]. Therefore, ATR-FTIR results suggested that the purification procedure did not induce any change on the chemical characteristics (i.e., chemical bonds) of Poloxamer®. Furthermore, the absence of new bands at  $3,300\text{ cm}^{-1}$ ,  $1,450\text{ cm}^{-1}$  and  $1,000\text{ cm}^{-1}$ , attributed to N-H stretching and bending vibrations and sulphate bending, respectively, confirmed the complete removal of the ammonium sulphate salt at the end of the purification step [Kadam et al. 2011].

Concerning Size Exclusion Chromatography analyses (Table S1), both the measured P407\_P Weight Average Molecular Weight ( $\bar{M}_w$ ) and Number Average Molecular Weight ( $\bar{M}_n$ ) showed a slight increase with respect to the control (i.e., not purified P407), thus suggesting a successful removal of the low molecular weight polymeric components [Fakhari et al. 2017]. Additionally, the slight reduction of the polydispersity index (D) further supported these observations. Moreover, the low standard deviation calculated for all the measured parameters confirmed a high repeatability of the purification process.

**Supplementary Table 1.** Number Average Molecular Weight ( $\overline{M}_n$ ), Weight Average Molecular Weight ( $\overline{M}_w$ ) and polydispersity index (D) measured for P407 and P407\_P samples belonging to three different batches.

| Macrodiol parameters |                       |                       |                   |
|----------------------|-----------------------|-----------------------|-------------------|
|                      | $\overline{M}_n$ (Da) | $\overline{M}_w$ (Da) | D                 |
| <b>P407</b>          | $8,612 \pm 62$        | $9,986 \pm 56$        | $1.200 \pm 0.002$ |
| <b>P407_P</b>        | $9,984 \pm 47$        | $10,883 \pm 48$       | $1.100 \pm 0.001$ |

These results were definitely confirmed by analyzing the molecular weight distribution profiles (figure S3). Indeed, both average spectra showed the characteristic bimodal molecular weight distribution profile ascribed to the concurrent presence of PEO-PPO-PEO and PEO-PPO triblock and diblock copolymers, respectively. However, compared to P407, P407\_P spectrum showed a sharp decrease in the intensity of the peak centered at 5,600 Da, i.e., the band attributed to the lower molecular weight fraction. On the other hand, no differences were registered for the higher molecular weight component (i.e., the triblock PEO-PPO-PEO). Hence, although a complete removal was not achieved (i.e., approx. 60% of the total diblock content), the purification procedure was effectively able to considerably reduce the amount of diblock copolymers while preserving PEO-PPO-PEO fraction in accordance with Fakhari et al. [Fakhari et al. 2017].

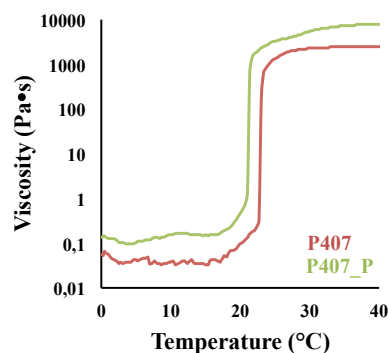


**Supplementary Figure S3.** Normalized Refractive Index (RI) signal as a function of Molecular weight  $M_i$  measured for P407 (red spectrum) and purified P407\_P (green spectrum).

### 2.1.2 Rheological characterization

Due to the alternation of hydrophilic (i.e., PEO) and hydrophobic (i.e., PPO) segments, polymers belonging to the Poloxamer® family show a temperature-driven chain arrangement into organized micelles with a hydrophobic core and a hydrophilic shell [Cespi et al. 2014; Ali Ibrahim et al. 2012]. To investigate hydrogel gelation mechanism upon PEO-PPO diblock removal, temperature ramp test within 0 °C - 40 °C, strain sweep test at physiological temperature and frequency sweep tests at 25 °C, 30 °C and 37 °C were performed on P407\_P samples (25% w/V). P407 sol-gel systems were prepared at the same concentration and analyzed according to the same protocols as control condition.

As illustrated in figure S4, the viscosity of both the analyzed systems initially slightly decreased as a function of temperature, reaching a minimum value that was measured to be 0.04 Pa·s and 0.15 Pa·s for P407 and P407\_P solutions, respectively. This remarkable lower viscosity value measured for P407 system could be attributed to the presence of low molecular weight chains [Fakhari et al. 2017]. Indeed, PEO-PPO diblocks could probably weaken the hydrophobic interactions between the polymeric chains, thus lowering the viscosity of the system [Fakhari et al. 2017].

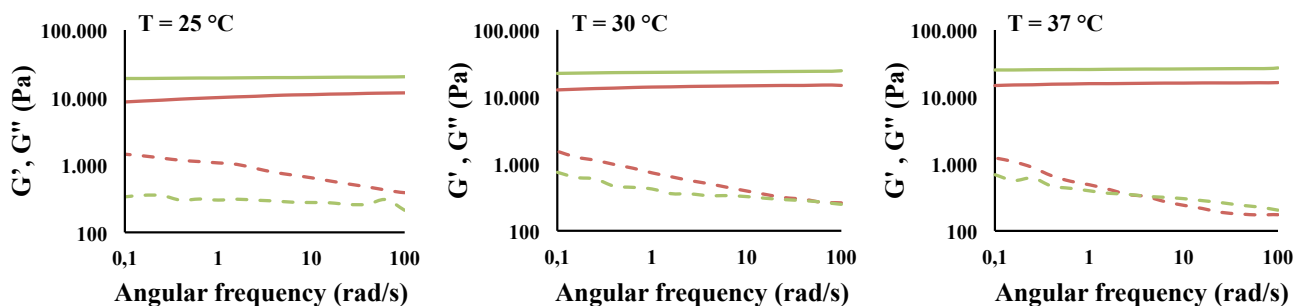


**Supplementary Figure S4.** Viscosity profiles *versus* temperature during the sol-to-gel transition as analyzed through temperature ramp test performed on P407 (red) and P407\_P (green) solutions at 25% w/V concentration.

The temperature at the minimum of viscosity was identified as the starting temperature of the gelation process ( $T_{\text{onset}}$ ). The measured  $T_{\text{onset}}$  of P407\_P-based sol-gel system was slightly lower compared to that of P407-based formulation (i.e., 15.3 °C and 16.7 °C, respectively). Indeed, considering a fixed solution concentration, P407\_P samples were mainly composed by PEO-PPO-PEO triblock copolymer, which probably favored the nucleation of micelles with larger size than P407. This suggested that the critical micellar volume of 0.53 needed for the onset of the sol-to-gel transition [Boffito et al. 2016] was reached at a lower temperature for P407\_P hydrogel compared to P407-based one. Subsequently, in both systems a sharp viscosity increase was registered due to micelle nucleation, growth and progressive packing with conversion of the homogeneous fluid into a biphasic system. Finally, the viscosity reached a maximum value followed by a plateau upon further temperature increase for P407 sol-gel systems, thus suggesting the achievement of a complete

gelation transition. Conversely, P407\_P systems showed a further viscosity increase upon heating up to 40 °C. This different behavior could be attributed to the formation of bigger micelles, which initially enhanced the gelation process but then, hindered gel formation as they more barely arranged into an organized network. Hence, additional heating was required to P407\_P systems to achieve further dehydration of PEO blocks, which favored micelle packing, macroscopically resulting in a viscosity plateau. Additionally, viscosity of P407\_P solution and hydrogel was higher than for P407-based system, due to the presence of triblock copolymer chains instead of a mixture of triblock and diblock copolymers.

To study the process of gel formation and development upon temperature increase and the influence of PEO-PPO diblock removal on polymeric chain arrangement into micelles and their packing into a gel network, frequency sweep tests were performed on both P407 and P407\_P sol-gel systems at 25 °C, 30 °C and 37 °C (figure S5). Conventionally, the sol phase is characterized by  $G'$  values lower than  $G''$  ones. On the contrary, when  $G'$  values are at least one order of magnitude higher than  $G''$  ones and both moduli are frequency-independent, the system is considered to be in the gel phase. Based on these considerations, both systems resulted to be in the gel state irrespective of the analyzed temperature. However, P407\_P formed stronger gels at each tested temperature as the differences between the storage and the loss moduli were measured to be significantly higher with respect to the control (Table S2). These observations could be attributed to the stronger hydrophobic interactions occurring in the absence of PEO-PPO by-products, in agreement with Fakhari et al. [Fakhari et al. 2017], and to a more regular structure characterized by the presence of chains with higher molecular weight.

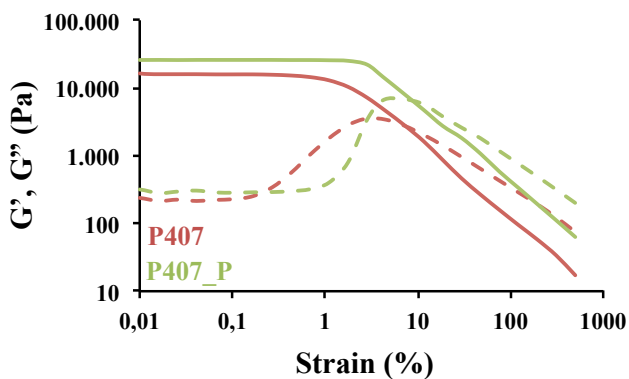


**Supplementary Figure S5.** Storage ( $G'$  - continuous line) and loss ( $G''$  - dashed line) moduli registered for P407 ( $G'$ ,  $G''$  - red) and P407\_P ( $G'$ ,  $G''$  - green) gels at 25 °C, 30 °C and 37 °C.

**Supplementary Table 2.** Differences between the storage ( $G'$ ) and the loss ( $G''$ ) moduli measured at 100 rad/s for P407 and P407\_P gels analyzed at 25 °C, 30 °C and 37 °C.

|               | $\Delta G_{100\text{rad/s}}$ (Pa) |         |         |
|---------------|-----------------------------------|---------|---------|
|               | @ 25 °C                           | @ 30 °C | @ 37 °C |
| <b>P407</b>   | 7,130                             | 11,200  | 13,600  |
| <b>P407_P</b> | 18,800                            | 21,700  | 24,100  |

Lastly, strain sweep tests (figure S6) performed on P407 and P407\_P gels reported similar trends of storage and loss moduli measured in the linear viscoelastic range as a function of applied deformation (Table S3). However, P407\_P gel showed a higher critical deformation compared to P407-based sample (i.e., 3.5 % vs. 2.3 %), thus suggesting slightly improved mechanical behavior of P407\_P.



**Supplementary Figure S6.** Storage ( $G'$  – continuous line) and loss ( $G''$  – dashed line) moduli registered as a function of applied deformation in the range 0.01% - 500% for P407 (red) and P407\_P (green) sol-gel systems.

**Supplementary Table S3.** Storage ( $G'$ ) and loss ( $G''$ ) moduli at 0.01% strain and critical deformation ( $\gamma_{\text{break}}$ ) measured for P407 and P407\_P sol-gel systems.

|               | Gel parameters |            |                             |
|---------------|----------------|------------|-----------------------------|
|               | $G'$ (Pa)      | $G''$ (Pa) | $\gamma_{\text{break}}$ (%) |
| <b>P407</b>   | 16,000         | 242        | 2.3                         |
| <b>P407_P</b> | 25,900         | 326        | 3.5                         |

### 3 Low Field Nuclear Magnetic Resonance spectroscopy

**Supplementary Table 4.** Mean spin-spin relaxation time  $T_{2m}$  values measured for CHP407 and CHP407\_P sol-gel systems at different time points.

|                 | Mean spin-spin relaxation time $T_{2m}$ (ms) |         |         |          |
|-----------------|--|---------|---------|----------|
|                 | t=0 min                                      | t=4 min | t=8 min | t=10 min |
| <b>CHP407</b>   | 1,277  | 1,471   | 1,523   | 1,560    |
| <b>CHP407_P</b> | 1,106  | 1,231   | 1,259   | 1,259    |

### 4 References

Boffito, M.; Pontremoli, C.; Fiorilli, S.; Laurano, R.; Ciardelli, G. and Vitale-Brovarone, C. (2019) Injectable thermosensitive formulation based on polyurethane hydrogel/mesoporous glasses for sustained co-delivery of functional ions and drugs. *Pharmaceutics* 11, 501-521.

Kadam S. S.; Mesbah, A.; Windt, E. and Kramer, H. J. M. (2011) Rapid online calibration for ATR-FTIR spectroscopy during batch crystallization of ammonium sulphate in a semi-industrial scale crystallizer. *Chem. Eng. Res. Des.* 89, 995-1005.

Fakhari, A.; Corcoran, M. and Schwarz, A. (2017) Thermogelling properties of purified poloxamer 407. *Heliyon* 3, 1-26.

Cespi, M.; Bonacucina, G.; Pucciarelli, S.; Cocci, P.; Perinelli, D. R.; Casettari, L.; Illum, L.; Palmieri, G.F.; Palermo, F.A. and Mosconi, G. (2014) Evaluation of thermosensitive poloxamer 407 gel systems for the sustained release of estradiol in a fish model. *Eur. J. Pharm. Biopharm.* 83, 1-8.

Ali Ibrahim, E. S.; Ismail, S.; Fetih, G.; Shaaban, O.; Hassanein, K. and Abdellah, N.H. (2012) Development and characterization of thermosensitive pluronic-based metronidazole in situ gelling formulations for vaginal application. *Acta Pharm.* 62, 59-70.